Meng, Weina and Garnett, Martin C. and Walker, David A. and Parker, Terence L. (2016) Penetration and intracellular uptake of poly(glycerol-adipate)nanoparticles into 3-dimensional brain tumour cell culture models. Experimental Biology and Medicine, 241 (5). pp. 466-477. ISSN 1535-3702

Penetration and intracellular uptake of poly(glycerol-adipate) nanoparticles into 3-dimensional brain tumour cell culture models

Weina Meng[1,2], Martin C. Garnett[1*], David A. Walker[3], Terence L. Parker[2†]
[1]School of Pharmacy and [2]School of Life Sciences, University of Nottingham, Nottingham, NG7 2RD, UK; [3]Queen's Medical Centre, Nottingham, NG7 2UH, UK

† In memory of Dr T.L. Parker deceased 15 October 2013

*Corresponding author Dr M C Garnett
E-mail: martin.garnett@nottingham.ac.uk
Tel: 0044 (0)115 951 5045 Fax: 0044 (0) 115 951 5102

Key Words:
Bionanoscience, Polymer Nanoparticles, Brain, Tumor models.
Journal Category: Bionanoscience
Declaration of conflicting interests: None declared
Funding: This research received no specific grant from any funding agency in the public commercial or not for profit sectors.

Author contributions
All authors participated in design, interpretation of the studies and analysis of the data and review of the manuscript; WM, MCG, and TLP conceived and designed the experiments, and analysed data; WM performed experiments, and wrote the paper; WM, MCG, DAW, and TLP edited the manuscript.

Abstract
Nanoparticle (NP) drug delivery systems may potentially enhance the efficacy of therapeutic agents. It is difficult to characterise many important properties of NPs *in vivo* and therefore attempts have been made to use realistic *in vitro* multicellular spheroids instead. In this paper we have evaluated poly(glycerol-adipate) (PGA) NPs as a potential drug carrier for local brain cancer therapy. Various 3-dimensional (3-D) cell culture models have been used to investigate the delivery properties of PGA NPs. Tumour cells in 3-D culture showed a much higher level of endocytic uptake of NPs than a mixed normal neonatal brain cell population. Differences in endocytic uptake of NPs in 2-D and 3-D models strongly suggest that it is very important to use *in vitro* 3-D cell culture models for evaluating this parameter. Tumour penetration of NPs is another important parameter which could be studied in 3-D cell models. The penetration of PGA NPs through 3-D cell culture varied between models, which will therefore require further study to develop useful and realistic *in vitro* models. Further use of 3-D cell culture models will be of benefit in the future development of new drug delivery systems, particularly for brain cancers which are more difficult to study *in vivo*.

Introduction

There is increasing interest in using NP delivery systems as novel treatments in cancer. The rationale for these delivery systems is based on the exploitation of differences between tumour and normal cells. However, existing cell culture methodologies are not sufficiently complex to model these differences, Traditional cell culture using 2-D monolayer methods has not even been particularly useful in assessing the efficacy of traditional therapeutic reagents, as *in vitro* studies often fail to predict the efficacy of these agents in clinical trials (1). It is now apparent that the poor *in vitro* and *in vivo* correlation may partly be due to limitations of 2-D cell culture systems. In this paper we will therefore explore alternative models 3-D models for their potential in assessing some biological aspects of NP drug delivery systems being designed for brain tumour therapies.

Cell culture condition is a key factor affecting neuronal growth and differentiation, and thus affects the cellular response to therapeutic drugs. *In vivo*, neurons develop extensive branches, dendrites and nerve fibres or axons. The length of the axon varies from a few tens of micrometers to several meters (2) and neurons reach high densities; for example, in human cortex, there are approximately 10^5 neurons per mm (2,3). In addition, neurons are a type of cell whose normal function is highly dependent on their interaction with other cells, especially glial cells. Glial cells can influence proliferation and differentiation of neurons (4), and secrete diffusible factors that trophically support neurons (5,6). Conventional *in vitro* 2-D culture systems involve cells grown at low density for convenience, particularly for the ability to view cellular interactions more easily. Conventional cultures also tend to use single cell types. However, this may not produce an active environment where behaviour of neurons is truly representative. Cells *in vivo* grow in a 3-D tissue environment, in which cell-cell and cell-extracellular matrix (ECM) interactions, ECM proteins and soluble protein factors affect drug access to target cells (7-10) of different types and this needs to be accurately replicated in our *in vitro* models. Thus, 3-D cell culture methods offer distinct advantages over conventional 2-D cell culture models. The increasing use and availability of confocal microscopy facilitates the use of 3-D cultures because of the possibilities for viewing these more complex models and for 3-D reconstructions.

Investigations of differences in the properties of cells in 2-D versus 3-D cell culture were first made by cancer researchers. They found fundamental differences related to integrin signalling (11,12), cell polarity (11), gene expression (13,14) and apoptosis, which lead to different responses of cancer cells towards therapeutic drugs between 2-D and 3-D cell culture (11,15-17). A variety of systems (e.g. scaffold, hydrogel, multicellular spheroid, multilayer cell culture, and microfluidic devices and spheroids on a chip) have been developed to mimic physiological 3-D environments (18,19). Among these, multicellular spheroids have been widely used for several decades as a 3-D tissue culture model for evaluating therapeutic drugs in cancer research. Recent findings have also indicated that cells respond differently to tissue or cell culture derived 3-D matrices compared to pure collagen gels or flat tissue culture substrates (20). In this paper we have therefore concentrated on an organotypic brain slice and 3-D models which form spheroids in the absence of added ECM ingredients.

Drug delivery is important in cancer research to try and exploit differences between tumour and normal tissue. Many delivery systems are macromolecular e.g. drug carrier conjugates, antibodies or NP, e.g. liposomes, nanocapsules and matrix NPs. It is assumed that these drug delivery systems may be preferentially accumulated in tumour tissue due to leaky vasculature (21,22). However, we need to consider how NPs can penetrate through the tumour to individual target cells (23). We are particularly interested in nanoparticle delivery systems for local delivery, e.g. post surgical application, convective enhanced delivery delivery etc,. In these applications, mobility and penetration of nanoparticles through tumour tissue and

selectivity of uptake would be particularly important. How do size, shape, and surface properties affect the mobility of NPs through ECM and their penetration within tissue after NPs leave the circulation? Does the ECM around tumour cells differ from normal cells, and how does it affect movement and penetration of NPs? Is there any selectivity difference at the tissue and cellular level (24)? Endocytosis of drug delivery systems has been almost exclusively investigated in monolayer culture and consequently there has been little consideration of the effect of 3-D culture on interactions of drug delivery systems with cells.
Thus in the drug delivery area important questions such as accessibility to cells, and penetration by macromolecules and NPs should be addressed in 3-D cultures. An increasing number of references relating to drug delivery have applied multicellular spheroid models for assessing various drug delivery systems. Our previous study (25) indicated selectivity of fluorescent dye loaded Poly(glycerol-adipate) (PGA) NPs between tumour cells and brain cells in a 3-D *in vitro* co-culture brain tumour invasion model. However it lacked evaluation of effect of ECM on cellular uptake and mobility of PGA NPs in various 3-D cell culture models. In this paper we have studied the cellular uptake and mobility of Rhodamine B Isothiocyanate (RBITC) labelled PGA NPs in 2-D and different 3-D cell culture models, such as various spheroids, and organotypic brain slices in order to present the importance of using 3-D cell culture models and how they may benefit the future development of new drug delivery systems. These more accurate *in vitro* models are particularly important for tumours which are more difficult to evaluate *in vivo* such as the brain cancers in which we are interested.

Materials and methods

Materials and reagents: Poly(glycerol-adipate) (PGA) was provided by Dr. G.A. Hutcheon and Dr. S. Higgins (The Drug Delivery and Materials Science Research group, Liverpool John Moores University, U.K). Rhodamine B Isothiocyanate (RBITC) was purchased from Sigma-Aldrich (Poole, UK). 4′, 6-diamidino-2-phenylindole dilactate (DAPI) and LysoTracker Yellow were obtained from Invitrogen (Paisley, U.K.). The DAOY cell line was purchased from American Type Culture Collection (ATCC; Rockvillle, MD, USA). Mouse anti-rat CD11B primary monoclonal antibody (OX-42) was purchased from Autogen Bioclear Ltd. (Wilts, UK). Fluorescein horse anti-mouse IgG(H+L) secondary antibody was obtained from Vector laboratories (Vector Laboratories, USA). All medium components and reagents for cell culture were obtained from Invitrogen Life Techologies Ltd. (Paisley, UK). All other chemicals were from Sigma-Aldrich (Poole, UK).

NP preparation for cellular uptake

NPs were prepared and characterised as described in our previous study (26) Details on methods for polymer synthesis, properties of the polymer and nanoparticles can be also be found here (26 and references within). For all experiments of NPs in the study of cellular uptake, PGA NPs were coated by addition of 1% polysorbate-80 to give a final concentration of 0.1% and passed through a syringe filter (0.2µm, Vivascience, Gemany) to sterilize the NP suspension.

Monolayer cell culture

DAOY, a human cerebellar medulloblastoma cell line, was maintained on Minimum Essential Medium (MEM) supplemented with 15% Fetal Bovine Serum (FBS), 200mM L-glutamine, 0.1mM non-essential Amino Acids, 1.0mM sodium pyruvate, 7.5% sodium bicarbonate solution at 37°C and 5% CO_2. Mixed brain cells were dissociated from whole brains of E-18 Wistar rats (Biomedical Sciences Unit, University of Nottingham) as follows: after whole brains were rapidly removed and immersed in ice-cold Hank's Balanced Salt Solution (HBSS) containing 10mM HEPES, brain tissues were gently minced into small pieces using a

scalpel. The tissue fragments were incubated with 2.5% trypsin (2ml) (Worthington Biochemical Corporation, NJ, USA) and HBSS (3ml) in 5% CO_2 incubator at 37°C. After 45 min of incubation, individual cells were gently dissociated from tissue fragments, cultured at a density at 1×10^6 cells/well or 0.5×10^6 cells /well in a 24-well tissue culture plate and maintained on MEM supplemented 10% NCS, 200mM L-glutamine, and 7.5% sodium bicarbonate solution at 37°C and 5% CO_2. Foetal brain cells were freshly derived for each experiment and were not passaged before use.

Spheroid culture

For DAOY spheroids, DAOY cells were grown in monolayer and detached from the substratum as described above. The individual cells (2 ml, 1×10^6 cells/ml) were cultured in DAOY culture medium in 25 ml screw top culture flasks (Scientific Laboratory Supplies, UK) and maintained at a constant rotation of 70 rev/min on an orbital shaker (Cole-Palmer, USA) at 37°C. Cultures were observed and medium was exchanged after 24 h of culture. Primary mixed brain spheroids were formed using two methods: (a) After individual cells were dissociated from E-18 rats, mixed brain spheroids were prepared and cultured as described previously for DAOY spheroids except that mixed brain spheroids were maintained on NCS supplemented MEM culture medium; (b) a second type of spheroid was formed spontaneously without any mechanical forces, in which high concentrations of individual cells (1ml, 5×10^6 cells/ml) were cultured in a 24-well plate and then individual cells reformed themselves into spheroids. The spheroids were maintained on NCS supplemented MEM culture medium.

Organotypic slice culture

Organotypic brain slices were prepared from 2-day-old Wistar rats. Cerebral cortices were cut into 400μm thick slices with a tissue chopper (McIlwain Tissue Chopper, Mickle Laboratory Engineering Co., Ltd., UK) under sterile conditions in a laminar flow hood. Three slices were then laid down on a Millicell-CM membrane insert (Millipore, Carrigtwohill, Co. Cork, Ireland), and the insert was placed in individual wells of 6-well plates. Medium (1ml) was added to the bottom of the culture plate (50). Slices were cultured in the same culture medium as mixed brain cells at 37°C with a 5% CO_2 incubator.

Cellular uptake of RBITC labelled NPs

For DAOY cells in 2-D culture, cells were plated at a density of 1×10^6 cells per 25 cm^2 tissue culture flask and allowed to attach for 24 h. To study the effect of incubation time on cellular NP uptake, cells were incubated in growth medium including 200μg NPs per 0.5×10^6 cells for different incubation time (from 15 min to 24 h). After cells washed with PBS three times, they were detached by Trypsin-EDTA for flow cytometry analysis.

For Mixed brain cells in 2-D culture, cells were seeded at 0.5×10^6 cells/ml per well in 24-well plates. For study of effect of incubation time on NP uptake, cells were incubated with growth medium including 200μg NPs for different incubation times. After cells were washed three times with PBS, cells were harvested by Trypsin-EDTA and prepared for flow cytometry study.

For spheroids in 3-D culture, after spheroids were formed, the growth medium was replaced with fresh culture medium containing NP suspension (200μg NPs/0.5×10^6 cells) and incubated for a series of incubation times (from 2 h to 24 h). At the end of the incubation period, spheroids were dissociated into single cells, washed three times with PBS and were studied by flow cytometry and confocal fluorescence microscopy.

For organotypic brain slices, cerebral cortices were maintained in culture medium for 14 days, then NP (200μg) suspension was added directly on the top of slices and incubated with slices for 24 h. LysoTracker Yellow (50nM) was added to each sample 1 h before the end of incubation time. Cerebral cortex slices were washed three times with PBS and fixed in 1% freshly prepared paraformaldehyde for microscopy.

Immunohistochemistry

Brain cerebral cortex slices were incubated with RBITC labelled NPs and LysoTracker (50nM), then were washed with Tris-HCl buffer (10mM, pH7.6) three times. Brain cerebral cortex slices were then fixed in periodate-lysine-paraformaldehyde fixative of McLean and Nakane (51) for 20 min at room temperature and processed for immunohistochemistry. Sections were incubated overnight with mouse anti-rat CD11B primary monoclonal antibody (Clone OX-42) (1:200 in Tris-HCl including 1%BSA) at 4°C. The monoclonal antibody CD11B recognizes the complement C3bi receptor which is expressed by brain macrophages and microglia (52-54). The sections were subsequently incubated with fluorescein horse anti-mouse IgG(H+L) secondary antibody (1:1000 in Tris-HCl with 1%BSA) for 1 h at room temperature and were observed using fluorescence microscopy (25).

Flow cytometry

Spheroids were treated with Trypsin-EDTA (1ml) at 37°C for 15 min to allow spheroid detachment. Individual cells were then gently dissociated from spheroids by using a glass Pasteur pipette. The intracellular fluorescence intensity was determined on a Beckman Coulter EPICS XL-MCL flow cytometer (Beckman Coulter Limited, Buckinghamshire, UK) using XL SYSTEM II™ software. Approximately 5000 cell events were evaluated for forward and side scatter characteristics to determine the trend of RBITC labelled NP taken up by cells.

Microscopy studies

Spheroids and slices were incubated with DAPI (300nM) for 30 min after samples were fixed. Samples were subsequently visualized and imaged under a Leica SP2 MP confocal microscope using a 476nm filter (LysoTracker), 488nm filter (fluorescein), 543nm filter (RBITC), and UV laser (DAPI). Standard settings for acquisition of images were used throughout this work to ensure that images obtained were comparable.

Penetration of NPs in 3-D cultures After spheroids and slices were incubated with NPs for 24 h, they were visualized under confocal fluorescence microscopy in the z-dimension with the same scan settings and z interval. For the spheroids, a similar z-section from the middle was selected and the mean fluorescence intensity (MFI) was measured from the periphery to the centre. Taking into account the spherical geometry of the spheroid, the MFI of comparable areas in these selected z-sections were determined. Organotypic slices were cultured on a membrane insert and the NP suspension was added onto the top flat surface of organotypic slice after 14-days in culture. A z-section from a similar middle level was also chosen to analyse MFI across the whole section of the organotypic slice. The MFI of each selected part of the section in the z-dimension was calculated using Image J and expressed as MFI per μm^2. One spheroid and organotypic slice were visualised each time and the experiment was carried out twice.

Results

Localisation of NPs in spheroids and organotypic slices

In the present study we are interested in the effects of both the dimensionality of the cell culture and multiple cell types on the penetration and cellular uptake of NP. We have therefore used a range of culture techniques including organotypic slices and spheroids produced in different ways. The PGA NPs used in this study have a size around 170 nm and have previously been reported to be taken up into DAOY medulloblastoma cells in monolayer culture (26). Throughout the study these NPs have been rhodamine labelled to allow easy identification.

The intracellular endocytic compartment of cells can be labelled using LysoTracker dye, which accumulates in acidic compartments. In Figure 1, using a control organotypic cerebral cortex slice which has not been exposed to NPs, it can be seen that the lysosome

compartments of these cells are small diffuse and not very prominent. Despite the low level and diffuse nature of the lysosomal compartment, it can still be seen localised near the nucleus in its characteristic arrangement.

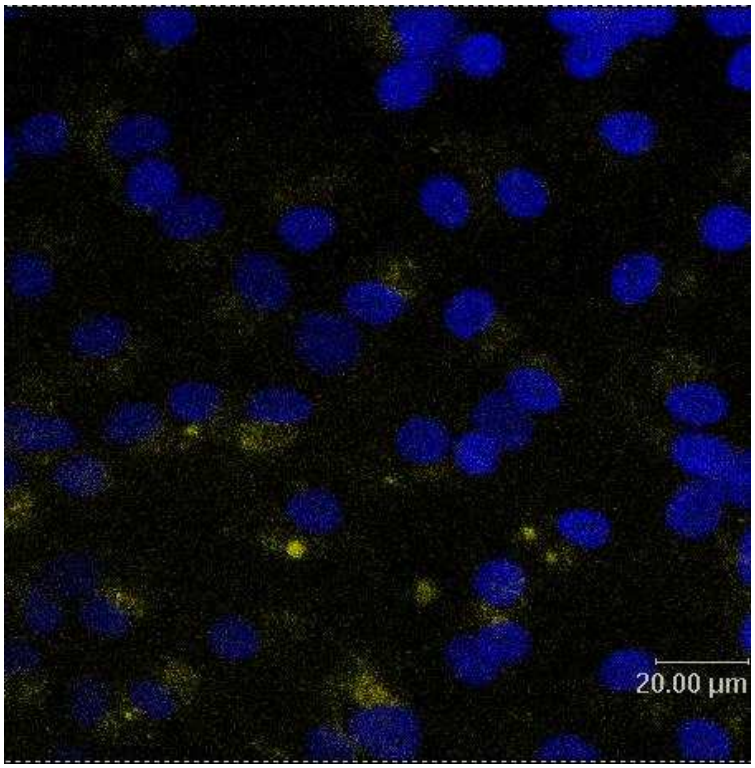

Figure 1 A confocal image of control organotypic cerebral cortex slices. Slices were incubated with 50nM LysoTracker Yellow for 2h. As can be seen, LysoTracker Yellow appears as very small yellow fluorescent dots in many cells.

In Figures 2 and 3 NPs have been added to the spheroids and organotypic slices respectively and the lysosome compartments were much more pronounced throughout both the spheroids and slices.
Figure 2 is a confocal image picture taken from a slice through the centre of a multicellular spheroid of DAOY cells in which the pattern of the NPs shows a strong resemblance to that of the lysoTracker dye. Combining these images gives an orange or yellow colour to most of the dots demonstrating localisation of most of the NPs within the lysosomal compartment.

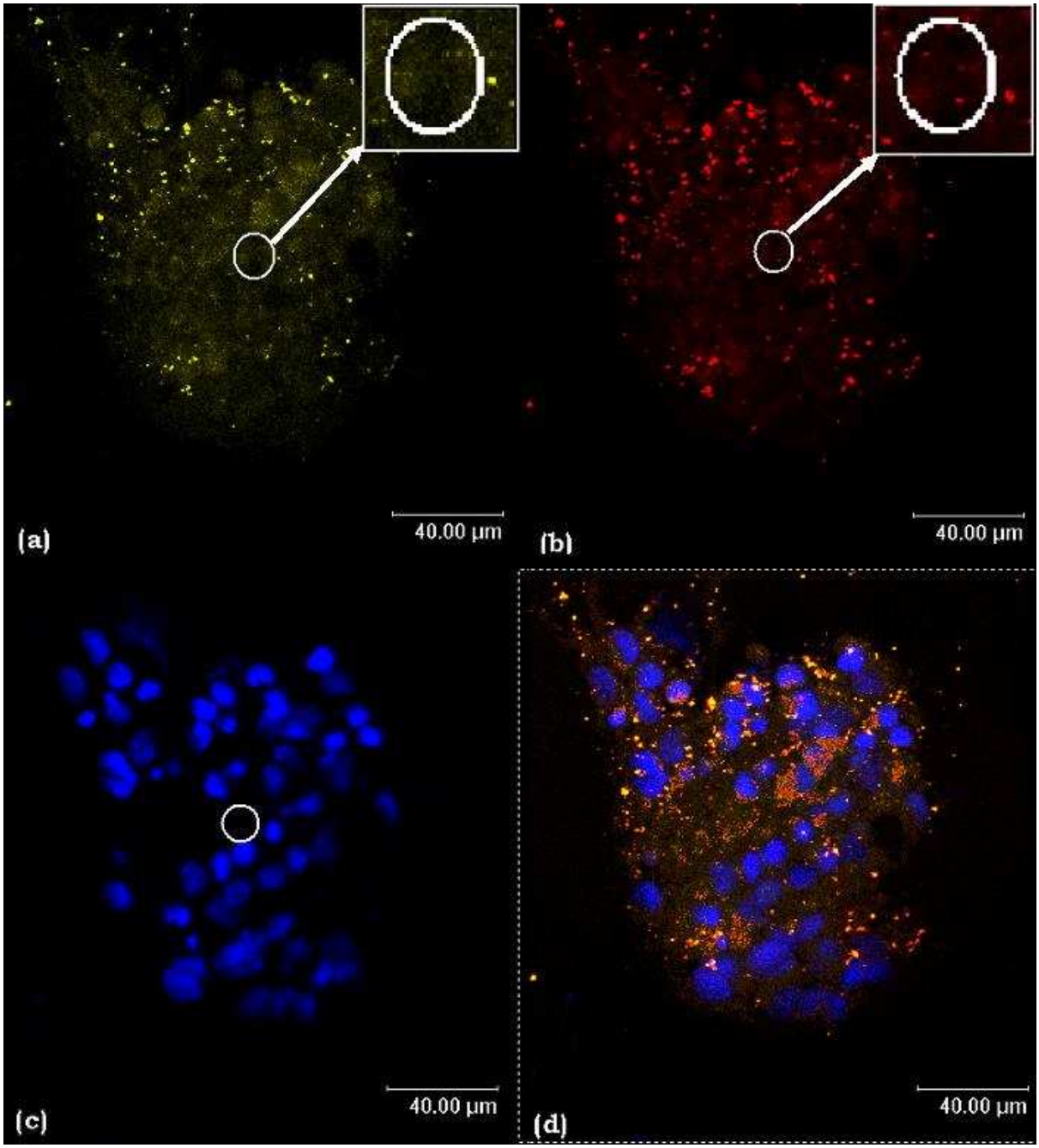

Figure 2 Confocal images showing localisation of RBITC labelled NPs within mixed neonatal brain spheroids: (a) yellow fluorescence from LysoTracker; (b) red fluorescence from NPs; (c) blue fluorescence from DAPI, a marker for nucleus; (d) co-localisation of red with yellow and blue fluorescence. The majority of NPs were taken up by brain cells and into the lysosome compartment and only a few NPs could be found localised in the interstitial compartment (white circle).

Closer examination (as indicated within circles and enlargements) reveals a few yellow dots of a lysosomal compartment with few NPs present, but also a few red dots which represent NPs outside of the lysosomal compartment. These may represent uptake into the cell cytoplasm, but as they are some distance from the blue DAPI stained nuclei they are much more likely to indicate NPs still outside the cells in the interstitial compartment. Figure 3 which is a similar confocal image of a brain slice shows a lower density of both red and yellow dots, but overall gives a similar picture of NP uptake.

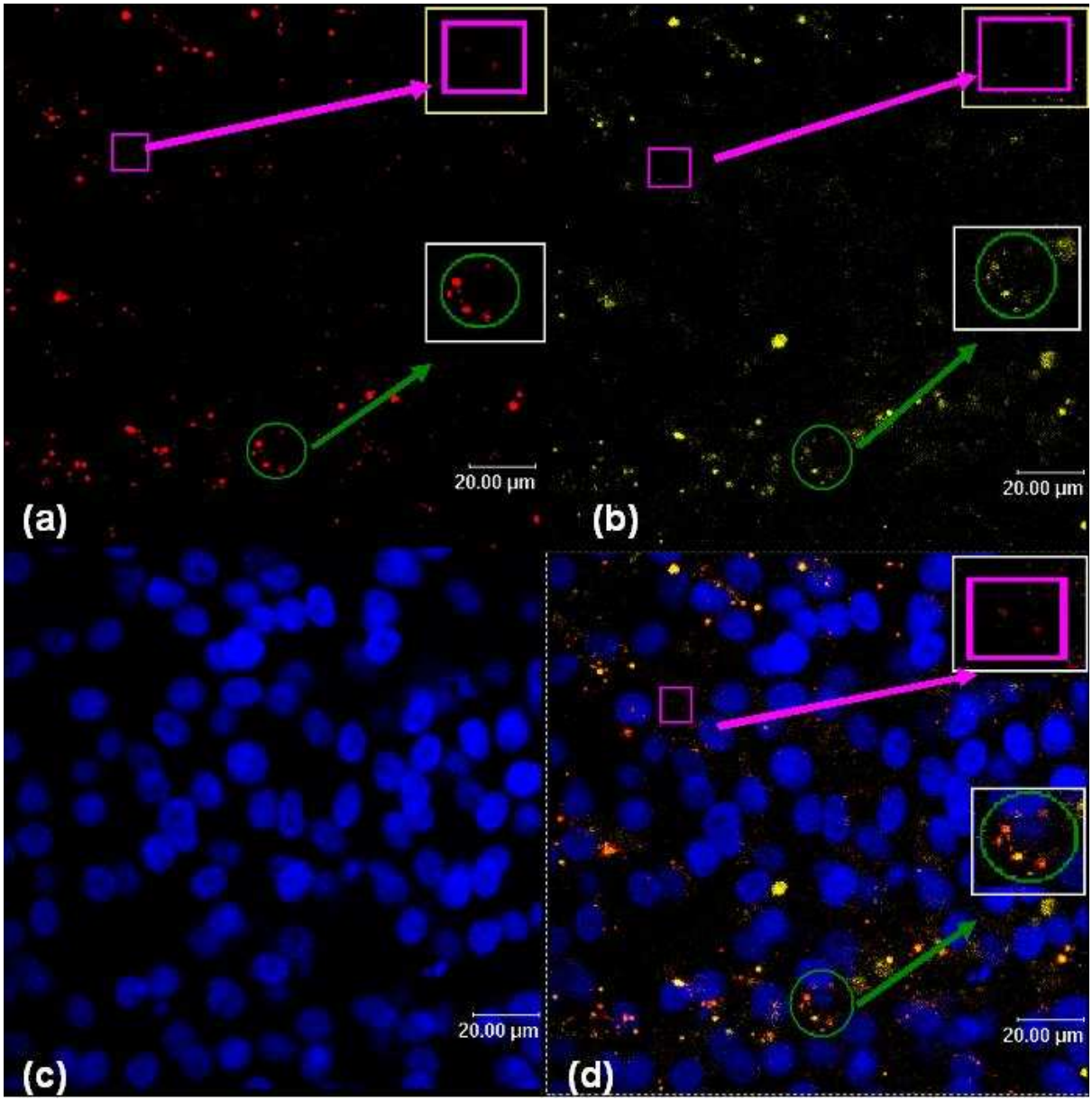

Figure 3 Confocal images of RBITC labelled NPs taken up by organotypic rat cerebral cortex slices: (a) red fluorescence from NPs; (b) yellow fluorescence from LysoTracker Yellow; (c) blue fluorescence from DAPI; (d) combined picture of red with yellow and blue fluorescence. The majority of NPs were taken up by brain cells and sorted into the lysosomal compartment (green circle) and few NPs are localised outside of cells (pink square).

Effect of cell type and culture dimension on uptake of NPs

After spheroids or monolayer cultures were incubated with RBITC labelled NP suspension for various times, they were dissociated into individual cells and then immediately assayed by flow cytometry (Figure 4). Intracellular Mean Fluorescence Intensity (MFI) in both types of cell in 2-D and 3-D culture increased with an increase of incubation time. Looking first at the situation in 2-D culture (dashed lines, empty symbols) it can be seen that the rate of NP uptake into mixed neonatal brain cells (circles) was greater than that of DAOY cells (squares). However, in 3-D culture (solid lines, filled symbols), MFI of cells from DAOY spheroids was much higher than from DAOY cells in monolayer culture and also higher than

mixed neonatal brain cells in 2-D culture. In the uptake study of DAOY spheroids, intracellular MFI reached its plateau after 6h.

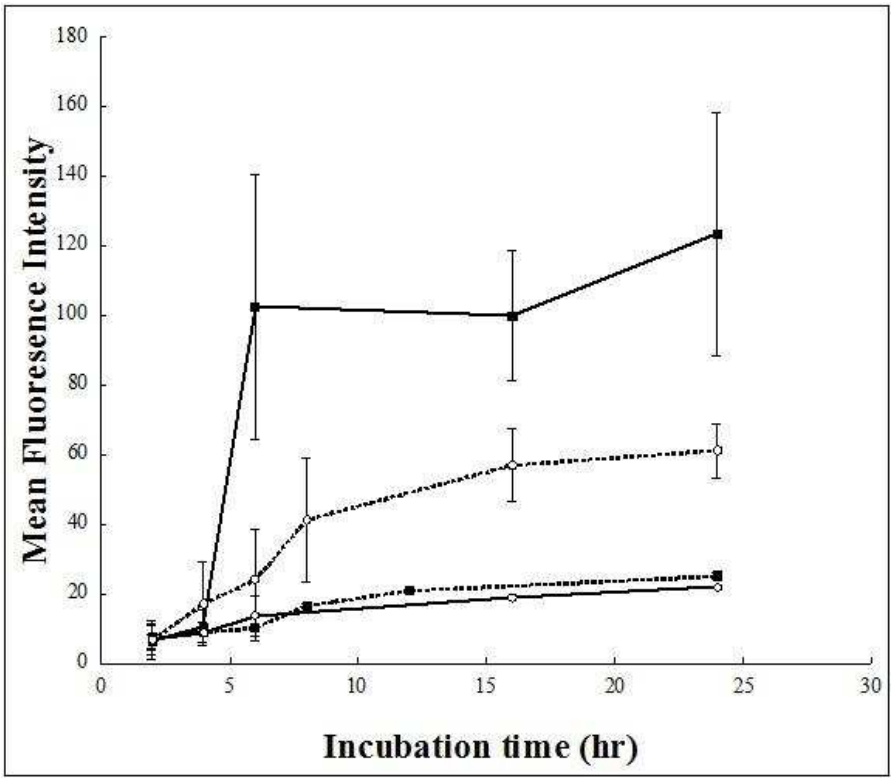

Figure 4 Time course for uptake of RBITC labelled NPs by DAOY cells and mixed foetal brain cells in different culture dimension. Uptake of NPs into DAOY cells (filled and square symbols was lower than in mixed neonatal brain cells (empty and round symbols) in monolayer culture (dashed lines), but in 3-D spheroids (continuous lines) culture this was reversed with a high uptake into DAOY spheroids and a low uptake into mixed neonatal brain spheroids. Mean ± SEM (n=3).

It was anticipated that 3-D nature of the cultures would affect penetration and uptake of particles and that some heterogeneity and time dependence of uptake may be expected. Consequently spheroid cultures of both mixed neonatal brain and DAOY cells treated with labelled NP were examined by confocal fluorescence microscopy. Fluorescence micrographs (Figure 5), which were taken from the middle of spheroids, were used to investigate the penetration and uptake pattern of NPs by spheroids formed by different type of cells. The pictures in Figure 5 are at slightly different magnification and have different scale bars so that the differences in uptake/penetration with time can be compared for each sequence of slides across the whole spheroid. These pictures are equivalent to the data in Figure 4 and show the qualitative differences in NP penetration and uptake between these different cell types. In the first several hours of incubation time (4 and 6 hours), the intensity of fluorescence in the periphery of spheroids was higher than that in the centre. With increased incubation time, the intensity of fluorescence in the centre of spheroids increased. However, the fluorescence intensity of mixed neonatal brain spheroids was much lower than that of DAOY spheroids after 24 h incubation time.

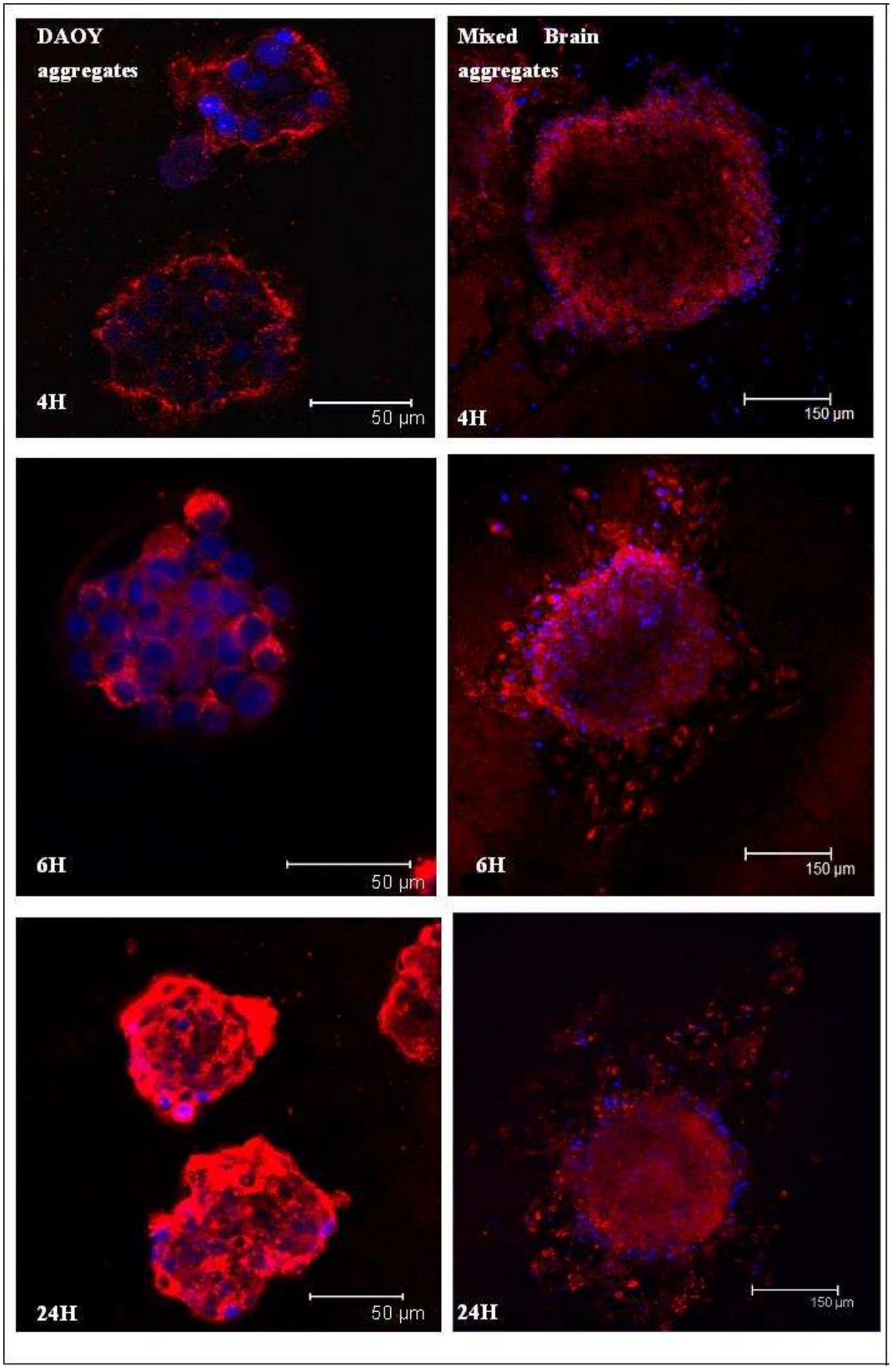

Figure 5 Time-dependent uptake and distribution of RBITC labelled NPs into DAOY and mixed brain spheroids. Uptake and distribution of NPs into DAOY spheroids is shown on the left column of images and into mixed brain spheroids in the right hand side images. The incubation time was monitored at 4h, 6h, and 24h. All pictures are optical sections through the centre of the aggregates.

Effect of cell culture models on penetration of NPs

The nature of the 3-D culture is also likely to influence penetration, so different 3-D culture models were also examined. We have compared the NP distribution pattern and penetration in a variety of 3-D combinations where the cells are grown in different types of spheroids or in slice culture. These different formats replicate to different degrees the 3-D microenvironment found *in vivo*. Figure 6 shows the distribution pattern and penetration of NPs in mixed neonatal brain spheroids prepared using two different methodologies and organotypic cerebral cortex slices.

Confocal fluorescence images in Figure 6 were taken from spheroids formed by the spontaneous method (a,e) and the rotation method (b,f) together with images from organotypic cerebral slices (d). Results from both methods resulted in spheroids that were completely formed and became well rounded and composed of highly compacted cells. The two types of spheroids had a similar size after 24 h growing on the glass coverslips and incubation with NPs, and thus a similar number of slices in the z-dimension so the z interval was kept constant throughout image acquisition.

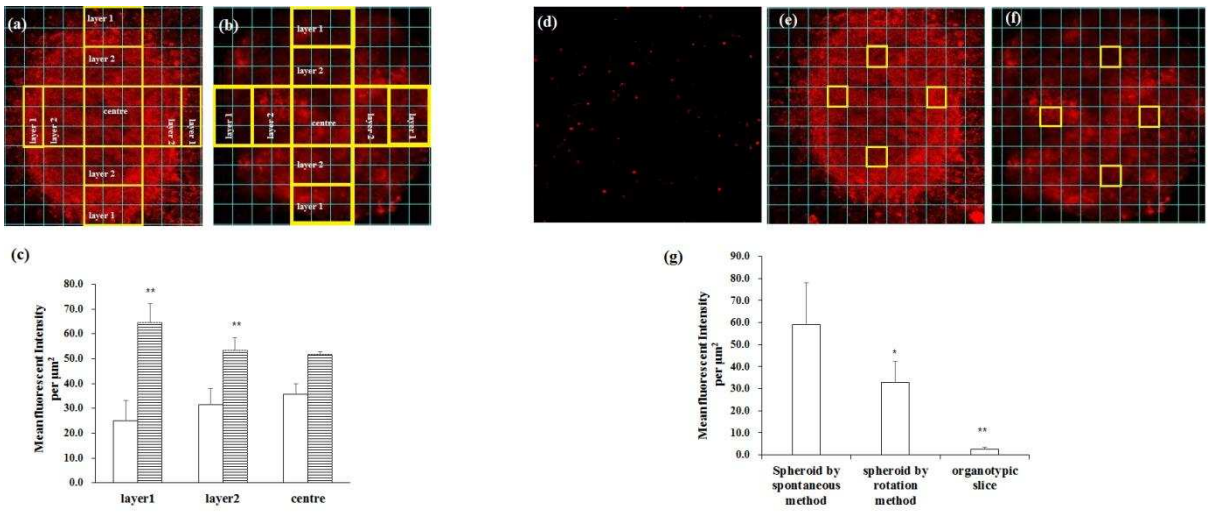

Figure 6 Confocal fluorescence images demonstrating penetration of NPs in 3-D cell culture: (a) showing the area of MFI measured in spontaneously formed mixed neonatal brain spheroids; (b) showing the area of MFI measured in spheroids formed by a rotation method; (c) a graph showing the MFI at the different sections through the spheroids. The MFI increased slightly from the periphery to the centre of the spheroids formed by the rotation method (empty columns) and the opposite trend was observed in spheroids formed spontaneously (horizontal lines). Student's t-test was used to determine the significance of differences in MFI between two types of spheroids. (** $p < 0.01$); (d) organotypic cerebral cortex slice; (e) showing the area of MFI measured in spontaneously formed spheroids; (f) showing the area of MFI measured in spheroids formed by rotation method; (g) graph comparing MFI in spheroids and organotypic slice at an equivalent penetration depth showing a decrease of MFI in the order spontaneous spheroid > rotation formed spheroid > organotypic slice. One way ANOVA was used to determine the significance of the differences in MFI between spheroids and organotypic slices (** $p < 0.01$, * $p < 0.05$)

The distribution pattern of red fluorescence in the inner region of spheroids was different between these two types of spheroids: red fluorescence in the sample of spheroids formed spontaneously (Figure 6a) was quite uniformly distributed; while in the sample of spheroids formed by the rotation method (Figure 6b), red fluorescence intensity was unevenly

distributed within spheroids. MFI in the middle section of the two different spheroid models were examined (a-c). To take account of the spherical geometry, the intensity of fluorescence was measured as shown by the grid from the periphery to the centre of spheroids (a,b) and expressed as MFI per μm^2. The resulting data plotted in Figure 6c shows that the MFI in spheroids formed by the rotation method was increased from the periphery to the centre while the MFI in spheroids formed spontaneously showed the opposite trend. The MFI in the periphery of spheroids formed spontaneously was significantly higher than in spheroids formed by the rotation method. The penetration of NPs into organotypic slices is shown in Figure 6d, and the penetration of NPs between between spheroids and organotypic slices were also compared. Organotypic slices were cultured on the membrane insert and NP suspension was added onto the top flat surface of organotypic slice after 14-day culture, whereas for the spheroids the NPs were in the solution surrounding the spheroids. Considering the spherical geometry of the spheroid and the flat surface of organotypic slice, the intensity of fluorescence measured as shown by the grids from half of radius of spheroids (Figure 6e and 6f, depth ~75μm) was used to compare with the intensity of fluorescence in the whole section of organotypic slice in the middle level of z-section (depth ~75μm). The organotypic slices showed a significantly lower level of intensity of fluorescence than the spheroids (Figure 6d and 6g). In the equivalent penetration depths among these culture models, the intensity of fluorescence was in decreasing order: spheroids formed spontaneously > spheroids formed by rotation method > organotypic culture.

Cell type study of NP uptake in organotypic cerebral cortex slices

Macrophages and professional phagocytes would be expected to be the cells mostly responsible for uptake of NPs within tissues. The normal cerebral cortex slices were first of all examined for the presence of Microglia or macrophages after 14 days culture using an antibody against CD11B as a marker for these cells (Figure 7a).

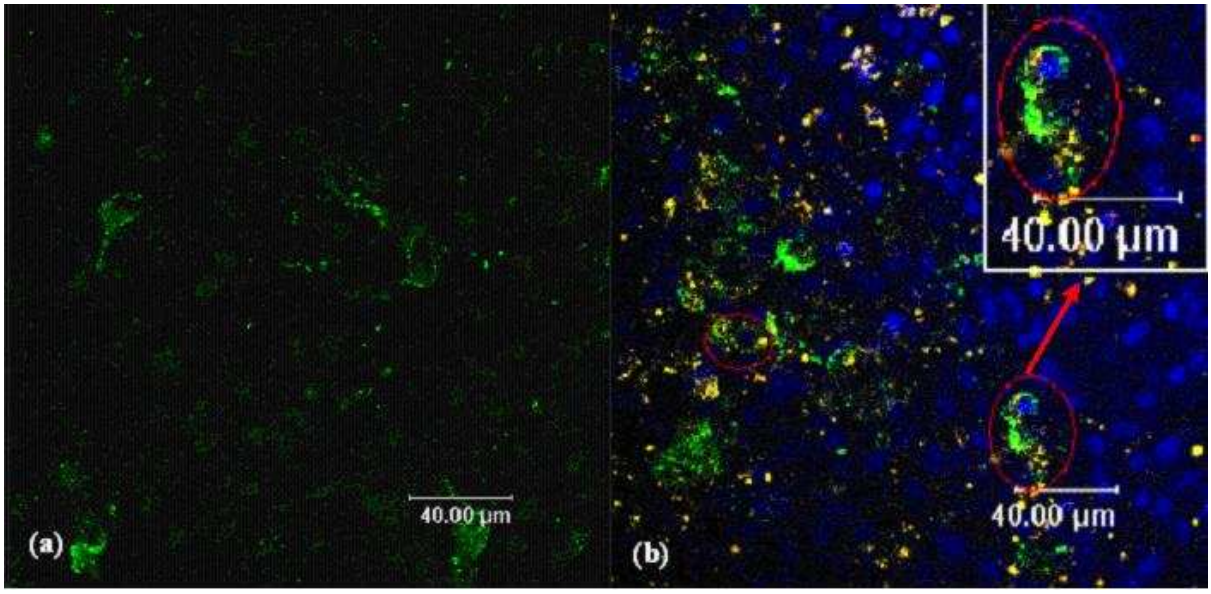

Figure 7 Confocal images demonstrating uptake of NPs taken up by organotypic rat cerebral cortex slices is cell type dependent: (a) slice with OX-42 labelling; (b) Slices incubated with NP suspension. Blue fluorescence from DAPI; Green fluorescence from monoclonal mouse OX-42 antibody, which labels macrophage cells; Orange fluorescence from co-location of NP (red) and LysoTracker (yellow). Few NPs were taken up by microglia (red circle).

This image clearly shows a good proportion of cells highlighted by this marker. Figure 7b illustrates the population of macrophages in organotypic slice culture exposed to the NP suspension is similar to the control sample (Figure 7a). It also shows that only a few orange fluorescent dots are localised intracellularly in CD11B labelled cells (green fluorescence), which suggested that not many NPs were recognized and taken up by brain macrophages or microglial cells, in contrast to the relatively higher uptake in some other unmarked cells within the slice.

Discussion

We have investigated a number of 3-D cell culture systems to assess their potential to give improved information on the performance of drug delivery systems using NPs prepared from the biodegradable polymer PGA. We have previously shown that PGA NPs are readily endocytosed by DAOY cells in monolayer culture (26). Here, we first wish to confirm endocytosis in 3-D mixed cell cultures. To understand the micrographs showing endocytosis, we first need to determine how the lysosomal compartment of cells appears in the absence of endocytic uptake.

Mixed neonatal brain spheroids and organotypic slices were incubated with NPs in the presence of LysoTracker Yellow which is colourless at neutral pH, but has a yellow fluorescence at acidic pH. LysoTracker Yellow freely permeates cell membranes, accumulating and becoming visible in acidic organelles in living cells. The control confocal fluorescence micrograph of cells not treated with NPs showed that in these cells the lysosomal compartment was minimally visible, with the very small dots of yellow indicating very small acidic vesicles. After cells were treated with NPs, it was observed that NPs were selectively taken up by some brain cells with most NPs sorted into the lysosome compartment and only a few NPs remaining localised in the ECM. The large increase in size of the lysosomal compartment after NP administration was also noted. Compared with control sample, it could be deduced that NP uptake increased the prominence of the compartment size of lysosomes. The large intracellular yellow fluorescent patches matched with large red fluorescent patches of red representing large amounts of NPs filling the lysosomes. The distribution of NP uptake was heterogeneous in both the spheroids and organotypic slices reflecting the mixture of cell types present in these cultures. It is important in studies that we are sure that the fluorescent label remains within the NPs so that we are not seeing leakage between cells. This has been demonstrated in other work by us, which showed that RBITC is retained within PGA NPs with a relatively slow release rate (26).

Quantification of NP uptake is important for drug delivery systems to ascertain whether there is any selective advantage between normal and tumour cell cultures. Our study showed that intracellular fluorescence intensity was about 5 times higher in DAOY spheroids than mixed neonatal brain spheroids while in monolayer culture mixed brain cells took up 2 times as many NP as the DAOY cells (Figure 4). The reasons why 3-D culture should enhance endocytosis by tumour cells but reduce it in normal cells is not immediately obvious. Mechanical tension generated between ECM and the cytoskeleton plays an important role in the regulation of cell growth, differentiation, ion channel activity, transmembrane receptor localisation at the plasma membrane of cells (27) and gene expression (28). In contrast to a 2-D substrate, cytoskeletal organization in spheroids has less mechanical stress. Closely packed spheroids increase cell-cell interactions and communication which have been found to

influence response of cells to drugs (29). Many studies have revealed increased specific activities of various lysosomal enzymes, such as β-glucuronidase, β-N-acetylglucosaminidase, and acid phosphatase in solid tumours than in their tissues of origin (30). Pinocytosis has previously been suggested as a mechanism for selective delivery to cancer cells based on studies of uptake of labelled proteins into tumours *in vivo* although *in vitro* cell culture studies did not show a consistent increase in pinocytosis rates (31 and references within). In our studies, 3-D culture was necessary to demonstrate an increased endocytosis into tumours as noted in these earlier *in vivo* studies, and may explain why a similar result was not seen in earlier *in vitro* studies using 2-D culture. A difference has been reported in the rate of uptake of nanomicelles into MDCK cells compared to various tumour related cell lines. Here a lower rate of endocytosis is seen in the confluent MDCK cells which is dependent on the formation of polarised epithelial cell layers due to loss of the caveolae mediated uptake pathway. This is probably just related to epithelial function (32). Cell cycle phase also influences rate of endocytosis in 2-D cell culture (33). However, in this case the difference between the highest and lowest rates of uptake is reported to be only double, so is unlikely to account for more than a fraction of the difference seen in our studies. Studies on mechanisms of cellular uptake and whether these are different under different culture conditions and in different types of cells will be investigated in future work.

To understand the properties of drug delivery systems, it is also important to determine how far NPs may penetrate into tumours for therapy. *In vitro* 3-D cell models may offer an opportunity to study such penetration and how it varies between different NP formulations more readily. In the present work we have studied the penetration of NPs into organotypic slices and spheroids produced by two different methods. Direct observation of spheroids by confocal fluorescence microscopy (Figure 6) showed that different methods of spheroid preparation affected the penetration of NPs through spheroids with the rotation method producing spheroids which showed a less effective penetration than spontaneously formed spheroids. Also penetration rate of NPs in spheroid models was faster than in organotypic slice culture (Figure 6). We should note that in addition to the tissue and ECM having an effect on the penetration of NPs, there may be some underestimation of penetration at increasing depth sections due to light attenuation during confocal microscopy. Once NPs were incubated with spheroids and slices, penetration of NPs through 3-D cell culture models was likely to be limited by the surface charge of NPs binding to cell surfaces and to ECM, by ECM protein density, and width of cell-cell junctions (34). The different preparation methods of two types of spheroids and organotypic brain slices might lead to different effects on the protein/polysaccharide concentration (35,36), viscosity of the medium (37) and size of the water channels in the interstitial spaces, width of intercellular gaps, the matrix charge and therefore ECM composition. ECM represents a major barrier to drug delivery systems (38). During tumour development, the presence of neutral collagen decreases and the content of negatively charged hyaluronan markedly increases (39). This can potentially influence the penetration rate of NPs via electrostatic repulsion forces. Therefore NP penetration rate and location within tumour will mainly depend on ECM composition, NP size, surface charge and surface coating (40,41). This is supported by a recent publication (42). The results from either of these spheroid models could be useful in relative studies comparing penetration of different NP delivery systems. However, we believe that the slower and lower penetration in the organotypic slices is much more representative of normal tissue in vivo.

The steric stabilisation provided by polysorbate 80 may also affect the penetration of these NPs. Polysorbate 80 is a non ionic surfactant which has both hydrophobic and hydrophilic moieties in its structure. The hydrophobic portions bind to the NP and present the hydrophilic components at the surface which would be expected to provide a low level of steric stabilisation. This alters NP surface properties such as surface charge and surface

hydrophobicity/hydrophilicity. The steric stabilisation of PEG chains appears to reduce penetration of liposomes (40,41). However, good penetration through spheroids was seen by our NPs. This may be due to the nature of the surface coating with short branched PEG chains of polysorbate 80. Also, good penetration of sterically stabilised NPs *in vivo* has previously been reported for intradermally administered small NPs (43), strongly suggesting that penetration of small NPs with a surface PEG layer through tissues does also occur *in vivo*, but that penetration is size dependent.

The mixed neonatal brain spheroids and organotypic brain slices used in our studies also revealed further information about differential uptake between cell types. Confocal images of co-localisation of NPs (Figure 2 and 3) clearly suggested that NP uptake was dependent on cellular type which was seen in both spheroids and organotypic cultures. It is expected from the literature on NP biodistribution that the major cell types involved in uptake of particulate materials would be the cells of the mononuclear phagocytic system and the reticulendothelial system (44,45). Macrophages also constitute a large percentage of the cell population in tumours (46). We therefore wished to ascertain whether macrophages were involved in uptake of our polysorbate 80 coated PGA NPs studied in more realistic organotypic brain slice culture model. Immunohistochemistry was therefore used to investigate: (1) whether brain macrophages or microglia still exist in cerebral cortex after long term culture; (2) whether NPs would be taken up by these macrophages. Some brain macrophages and microglia were found in our slice culture model (Figure 7a) as expected, because it is reported that brain macrophages only disappear completely after the third postnatal week and microglia exhibit a gradual increase in number (47). Compared to significant NP uptake by some other cells, only a few NPs were taken up by macrophages or microglia in organotypic brain slice culture. It is not clear whether macrophages in tumour tissue will have the same specificity for particle uptake. Macrophages show significant plasticity during different phases of tumour development initially promoting neoplastic transformation and then switching to immunosuppression and supporting angiogenisis and metastasis (48). There was also clearly some uptake of NPs by cell types other than macrophages indicating some selectivity, and perhaps indicating that steric stabilisation of particles is not the only factor affecting uptake. Polysorbate 80 coated NPs have been reported to be transported across the blood brain barrier due to adsorption of a serum protein, apo E (49), and a similar mechanism for selectivity into different types of cells through adsorption of serum proteins could be operating in our case.

Overall these uptake studies have revealed a number of interesting findings. We have provided good evidence that detergent stabilised PGA NPs have differential endocytic uptake not only between tumour and normal cells, but also in the type of culture model whether in 2 or 3 dimensions. It was also noted that there appeared to be differences of endocytic uptake between different types of normal neonatal brain cells, although we did not identify the different types. We may also speculate that uptake is also likely to be dependent on the nature of the surface of NPs and may therefore differ between formulations. In addition, the apparent preferential NP penetration into tumour spheroids in comparison to normal tissue spheroids may be reflective of differences in the respective 3-D microenvironments. This may not be indicative of the tissues *in vivo* but at least in controlled laboratory conditions there appears to be a real difference between the two types of model. It is also clear that 2-D models are of limited relevance for *in vitro* studies of drug delivery function, and that further development and understanding of 3-D culture models may prove helpful in understanding interactions between tissues and drug delivery systems. Further studies will be required to define an *in vitro* 3-D model which is both convenient to use and evaluates potential for measuring NP endocytosis and penetration relevant to the *in vivo* situation.

Acknowledgments

This paper is dedicated to the memory of Dr T. L. Parker for all support and supervision during the whole work. The poly(glycerol-adipate) polymers used in this project were generated through a BBSRC funded collaborative project (Grant number 42/E19350) in a collaboration between University of Nottingham and Liverpool John Moores University. We would like to thank Dr S Higgins and Dr G Hutcheon for the synthesis and provision of these polymers. We would like to thank Dr P Kallinteri for technical asistance and advice in PGA NP preparation. The Children's Brain Tumour Research Trust in Nottingham provided funding for consumables and instrumentation.

Declaration of conflicting interests:

None declared

Funding:

This research received no specific grant from any funding agency in the public commercial or not for profit sectors.

References

1. Hickman JA, Graeser R, de Hoogt R, Vidic S, Brito C, Gutekunst M, van der Kuip H and IMI PREDECT Consortium. Three-dimensional models of cancer for pharmacology and cancer cell biology: capturing tumor complexity in vitro/ex vivo. *Biotechnol J* 2014;**9:**1115-1128
2. Brown AG. Nerve cells and nervous systems: An Introduction to Neuroscience. Springer-Verlag; London, 1991
3. Kandel ER, Schwartz JH, and Jessel TM. *Principles of neural science*, 3rd Edition, Prentice Hall International, London. 1991
4. Levitt P, and Rakic P. Immunoperoxidase localization of glial fibrillary acidic protein in radial glial-cells and astrocytes of the developing rhesus-money brain. *J Comp Neurol* 1980;**193:** 815-840
5. Banker GA. Trophic interactions between astroglial cells and hippocampal neurons in culture. *Science* 1980;**209:** 809-810
6. Selak I, Skaper SD, and Varon S. Pyruvate participation in the low molecular weight trophic activity for central nervous system neurons in glia-conditioned media. *J Neurosci* 1985;**5:**23-28
7. Pluen A, Boucher Y, Ramanujan S, McKee T, Gohongi T, di Tomaso E, Brown E, Izumi Y, Campbell R, Berk D, and Jain R. Role of tumor-host interactions in interstitial diffusion of macromolecules: Cranial vs. subcutaneous tumors. *Proc Natl Acad Sci* 2001;**98:** 4628-4633
8. Goodman T, Oliver P, and Pun S. Increased nanoparticle penetration in collagenase-treated multicellular spheroids. *Int J Nanomedicine* 2007;**2:** 265-274
9. Kim TH, Mount CW, Gombotz WR, and Pun SH. The delivery of doxorubicin in 3-D multicellular spheroids and tumors in a murin xenograft model using tumor-penetrationg triblock polymeric micelles. *Biomaterials* 2010;**31:** 7386-7397
10. Dilnawaz F, and Sahoo SK. (2013) Enhanced accumulation of curcumin and temozolomide loaded magnetic naoparticles executes profound cytotoxic effect in glioblastoma spheroid model. *Eur J Pharm Biopharm* 2013;**85:** 452-462
11. Lefevre F, Garnotel R, Georges N, and Gillery P. Modulation of collagen metabolism by the nucleolar protein fibrillarin. *Exp Cell Res* 2001;**271:** 84-93
12. Pouliot N, Connolly LM, Moritz RM, Simpson RJ, and Burgess AW. Colon cancer cells adhesion and spreading on autocrine laminin-10 is mediated by multiple integrin receptors and modulated by EGF receptor stimulation. *Exp Cell Res* 2000;**261:** 360-371
13. Spencer V, Xu R, and Bissell M. Gene expression in the third dimension: the ECM-

nucleus connection. *J Mammary Gland Bio Neoplasia* 2010;**15:** 65-71
14. Zschenker O, Streicheit T, Hehlgans S, and Corders N. Genome-wide gene expression analysis in cancer cells reveals 3D growth to affect ECM and processes associated with cell adhesion but not DNA repair. *PloS One* 2010;**7:** e3427
15. Sahai E. and Marshall CJ. Differing models of tumour cell invasion have distinct requirements for Rho/ROCK signaling and extracellular proteolysis. *Nat cell Biol* 2003;**5:** 711-719
16. Sacks PG, Oke V, and Mehta K. Antiproliferative effects of free and liposome-encapsulated retinoic acid in a squamous carcinoma model: monolayer cells and multicellular tumor spheroids. *J Cancer Res Clin Oncol* 1992;**118:** 490-496
17. Horning JL, Sahoo SK, Vijayaraghavalu S, Dimitrijevic S, Vasir JK, Jain TK, and Panda AK. 3-D tumor model for in vitro evaluation of anticancer drugs. *Mol Pharm* 2008;**5:** 849-862
18. Cukierman E, Pankov R, and Yamada KM. Cell interactions with three dimensional matrices. *Curr Opin Cell Biol* 2002;**14:** 633-639
19. Goodman T, Ng C, and Pun S. 3-D tissue culture systems for evaluation and optimization of nanoparticle-based drug carriers. *Bioconju Chem* 2008;**19:** 1951-1959
20. Cukierman E, Pankov R, Stevens DR, and Yamada KM. Taking cell-matrix adhesions to the third dimension. *Science* 2001;**294:** 1708-1712
21. Huang SK, Lee K-D, Hong K, Friend DS, and Papahadjopoulos D. Microscopic localisation of sterically stabilised liposomes in colon carcinoma-bearing mice. Cancer Res 1992;**52:** 5135-5143
22. Wu NZ, Da D, Rudoll TL, Needham D, Whorton R, and Dewhirst MW. Increased microvascular permeability contributes to preferential accumulation of stealth liposome in tumour tissue. *Cancer Res* 1993;**53:** 3765-3770
23. Jain RK. Delivery of molecular and cellular medicine to solid tumours. *Adv Drug Deliv Rev* 2001;**46:** 149-168
24. Emfietzoglou D, Kostarelos K, Papakostas A, Yang W-H, Ballangrud A, Song H, and Sgouros G. Liposome-mediated radiotherapeutics within avascular tumour spheroids: comparative dosimetry study for various radionuclides, liposome systems and a targeting antibody. *J. Nucl Med* 2005;**46**: 89-97
25. Meng W, Kallinteri P, Walker DA, Parker TL, Garnett MC. Evaluation of poly (glycerol-adipate) nanoparticle uptake in an *in vitro* 3-D Brain Tumour Co-Culture Model. *Exp Biol Med* 2007;**232:** 1100-1107
26. Meng W, Parker TL, Kallinteri P, Walker DA, Higgins S, Hutcheon GA, Garnett MC. Uptake and metabolism of novel biodegradable poly (glycerol-adipate) nanoparticles in DAOY monolayer. *J Control Release* 2006;**116:** 314-321
27. Janmey PA. The cytoskeleton and cell signaling: component localization and mechanical coupling. *Physiol Rev* 1998;**78:** 763-781
28. Chicurel ME, Chen CS, and Ingber DE. (1998) Cellular control lines in the balance of forces. *Curr Opin Cell Biol* 1998;**2:** 232-239
29. Oloumi A, Lam W, Banath JP, and Oliver PL. Identification of genes differentially expressed in V79 cells grown as multicell spheroids. *Int J Radiat Biol* 2002;**78:** 483-492
30. Allison AC. Lysosomes in cancer cells. *J Clin Pathol Suppl (R Coll Pathol)* 1974;**7:** 43-50
31. Trouet A, Deprez-de Campeneere and de Duve C. Chemotherapy through lysosomes with a DNA-daunorubicin complex. *Nature New Biology* 1972;**239:** 110-112
32. Sahay G, Kim JO, Kabanov AV, Bronich TK. The exploitation of differential endocytic pathways in normal and tumor cells in the selective targeting of nanoparticulate chemotherapeutic agents. *Biomaterials* 2010;**31:**923-933

33. Kim JA, Åberg C, Salvati A, Dawson KA. Role of cell cycle on the cellular uptake and dilution of nanoparticles in a cell population. *Nat Nanotechnol* 2011; **7:**62-68
34. Mehta G, Hsiao AY, Ingram M, Luker GD, and Takayama S. Opportunities and challenges for use of tumor spheroids as models to test drug delivery and efficacy. *J Control Release* 2012;**164:** 192-204
35. Margolis EK, and Margolis RU. Nervous tissue proteoglycans. *Experientia* 1993;**49:** 429-446
36. Novak U, and Kaye AH. Extracellular matrix and the brain: components and function. *J Chin Neurosci* 2000;**7:** 280-290
37. Hrabětová S, and Nicholson C. Contribution of dead-space microdomains to tortuosity of brain extracellular space. *Neurochem Int* 2004;**45:** 467-277
38. Jain RK. Delivery of molecular and cellular medicine to solid tumors. *Microcirculation* 1997;**4:** 1-23 Novak U, and Kaye AH. Extracellular matrix and the brain: components and function. *J Chin Neurosci* 2000;**7:** 280-290
39. Toole BP. Hyaluronan: from extracellular glue to pericellular cue. *Nat Rev Cancer* 2004;**4:** 528-539
40. Yuan F, Leunig M, Huang SK, Berk DA, Papahadjopoulos D, and Jain RK. Microvascular permeability and interstitial penetration of sterically stabilised (Stealth) liposomes in a human tumour xenograft. *Cancer Res* 1994;**54:** 3352-3356
41. Kostarelos K, Emfietzoglou D, Papakostas A, Yang WH, Ballangrud A, and Sgouros G. Binding and interstitial penetration of liposomes within avascular tumor spheroids. *Int J Cancer*2004; **112:** 713-721
42. Jiang X, Xin H, Gu J, Xu X, Chen S, Xie Y, Chen L, Chen Y, Sha X, and Fang X. (2013) Solid tumor penetration by integrin-mediated pegylated poly (trimethylene carbonate) nanoparticles loaded with paclitaxel. *Biomaterials* 2013;**34:** 1739-1746et
43. Moghimi SM, Hawley AE, Christy NM, Gray T, Illum L, and Davis SS. Surface engineered nanospheres with enhanced drainage into lymphatics and uptake by macrophages of the regional lymph nodes. *FEBS Lett* 1994;**344:** 25-30
44. Illum L, Thomas NW, and Davis SS. Effect of a selected suppression of the reticuloendothelial system on the distribution of model carrier particles. *J Pharm Sci* 1986;**75:** 16-22
45. Illum L, Jacobsen LO, Muller RH, Mak E, and Davis SS. Surface characteristics and the interaction of colloidal particles with mouse peritoneal macrophages. *Biomaterials* 1987;**8:** 113-117
46. Sutherland RM. Cell and environment interactions in Tumour microregions: the multicell spheroid model. *Science* 1988;**240:** 177-184
47. Milligan CE, Cunningham RJ, and Levitt P. Differential immunochemical markers reveal the normal distribution of brain macrophages and microglia in the developing rat brain. *J Comp Neurol* 1991;**314**: 125-135
48. Biswas SK, Sica A, and Lewis CE. Plasticity of Macrophage Function during Tumour Progression: Regulation by Distinct Molecular Mechanisms. *J of Immunology* 2008;**180:** 2911-2017
49. Kreuter J. Nanoparticulate systems for brain delivery of drugs. Adv Drug Del Reviews 2001;**47:** 65-81
50. Stoppini L, Buchs PA, and Muller D. A simple method for organotypic cultures of nervous tissue. *J Neurosci Methods* 1991;**37:** 173-182
51. McLean IW, and Nakane PK. Periodate-lysine-paraformaldehyde fixative a new fixative for immunoelectron microscopy. *J Histochem and Cytochem* 1974;**22:** 1077-1083

52. Perry VH, Hume DA, and Gordon S. Immunohistochemical localization of macrophages and microglia in the adult and developing mouse brain. *Neurosci* 1985;**15:** 313-326
53. Perry VH, and Gordon S. Macrophages and microglia in the nervous system. *TINS* 1988;**11:** 273-277
54. Robinson AP, White TM, and Mason DW. Macrophage heterogeneity in the rat as determined by two monoclonal antibodies MRC OX-41 and MRC OX-42, the latter recognizing complement receptor type 3. *Immunol* 1986;**57:** 239-247